INTERNATIONAL JOURNAL FOR NUMERICAL METHODS IN FLUIDS, VOL. 5, 1047–1057 (1985)

SHORT COMMUNICATION

CONSERVATIVE CALCULATIONS OF NON-ISENTROPIC TRANSONIC FLOWS

M. M. HAFEZ*

University of California, Davis, CA, U.S.A.

W. G. HABASHI*

Concordia University, Montreal, Quebec, Canada

AND

P. L. KOTIUGA†

Pratt & Whitney Canada Inc., Longueuil, Quebec, Canada

SUMMARY

The classical potential formulation of inviscid transonic flows is modified to account for non-isentropic effects. The density is determined in terms of the speed as well as the pressure, which in turn is calculated from a second-order mixed-type equation derived via differentiating the momentum equations.

The present model differs in general from the exact inviscid Euler equations since the flow is assumed irrotational. On the other hand, since the shocks are not isentropic, they are weaker and are placed further upstream compared to the classical potential solution. Furthermore, the streamline leaving the aerofoil does not necessarily bisect the trailing edge.

Results for the present conservative calculations are presented for non-lifting and lifting aerofoils at subsonic and transonic speeds and compared to potential and Euler solutions.

KEY WORDS: Transonic Flow Modified Potential Finite Elements Non-isentropic Flow Conservative Method

INTRODUCTION

The potential formulation has proved to be a useful tool for the design and analysis of transonic flows around practical aerodynamic configurations. There are, however, severe limitations since the flow is assumed to be irrotational and isentropic.

On the other hand, the exact inviscid model described by the Euler equations, which account for vorticity and non-isentropic effects, is more complicated and definitely more expensive to solve. For example, in three-dimensional calculations, a system of first-order equations in five variables has to be solved instead of a second-order equation in one variable for the potential. The boundary conditions are also more complicated. Despite the recent concentrated activity to develop efficient iterative procedures and accurate discretization techniques for the Euler equations, potential

---

* Consultant, Pratt & Whitney Canada Inc., Longueuil, Quebec, Canada.
† Aerodynamics Engineer.

0271–2091/85/121047–11$01.10

Received May 1985

calculations, when valid, are still more attractive in terms of both efficiency and accuracy. Therefore, there is an incentive to extend the range of validity of the potential formulation.

In this paper, a new potential model is presented where the flow is not necessarily isentropic. To calculate the non-isentropic losses, a second order mixed-type equation for the pressure is solved. The density is then determined in terms of both the pressure and the speed. Thus, the additional expenses are relatively minor.

Moreover, unlike the classical potential, the present model is useful for internal flows with prescribed back pressure, and in general the results are closer to the Euler solution.

In the following sections, previous methods where the entropy is explicitly calculated in terms of the Mach number upstream of the shock, are briefly reviewed and the details of the present method, where shocks are automatically captured, are presented. Numerical results are compared to potential and Euler solutions.

TRANSONIC SMALL DISTURBANCE EQUATION

For the sake of demonstrating the concept of the present model let us first discuss the small perturbation problems. Consider the expansion of the flux in terms of the velocity perturbation, assuming isentropic flow:

$$\rho(1+u)=\left\{1-\frac{\gamma-1}{2}M_\infty^2[(1+u)^2-1]\right\}^{1/(\gamma-1)}(1+u)$$
$$\simeq 1+(1-M_\infty^2)u-\tfrac{1}{2}M_\infty^2u^2[3-(2-\gamma)M_\infty^2]+\cdots \tag{1}$$

If the last term is approximated by $\frac{1}{2}M_\infty^2u^2(\gamma+1)$ the von Karman small disturbance equation reads

$$\{[(1-M_\infty^2)\phi_x-\tfrac{1}{2}M_\infty^2(\gamma+1)\phi_x^2]\}_x+\phi_{yy}=0. \tag{2}$$

Similarly, the momentum is given by

$$M=\rho(1+u)u+p=\frac{1}{\gamma M_\infty^2}+(1-M_\infty^2)\frac{u^2}{2}-[1-\tfrac{1}{3}(2-\gamma)M_\infty^2]M_\infty^2u^3+\cdots \tag{3}$$

and hence across an isentropic shock, assuming mass is conserved, the following relation is valid:

$$[\![M]\!]\simeq-\frac{M_\infty^2(\gamma+1)}{12}[\![u]\!]^3 \tag{4}$$

$[\![\ ]\!]$ denoting the jump in a quantity.

The drag in the small disturbance calculation can be represented by the integral of M along the shock.[1,2]

The jump condition admitted by a normal isentropic shock is simply

$$(1-M_\infty^2)-M_\infty^2(\gamma+1)\langle\phi_x\rangle=0 \tag{5}$$

where $\langle\phi_x\rangle=\frac{1}{2}(\phi_{x_u}+\phi_{x_d})$ is the average of the perturbation velocities upstream and downstream of the shock. In Reference 3, equation (5) is rewritten in the form:

$$1+\phi_{x_u}+\phi_{x_d}=a^{*2}. \tag{5'}$$

It is clear that (5′) is an approximation of the Prandtl relation where the second order ($\tau^{4/3}$) term $\phi_{x_u}\phi_{x_d}$ is neglected. It is also shown in Reference 3 that the vorticity ω is indeed of higher order ($\omega=O(\tau^{7/3})$); hence it is feasible to account for the entropy only and neglect the vorticity. A shock-fitting procedure is used, where the shock is assumed as an internal boundary with a Neumann boundary condition based on the Prandtl relation, i.e.

$$\phi_{x_d} = \frac{a^{*2}}{1 + \phi_{x_u}} - 1. \tag{6}$$

In this calculation, the momentum is conserved and the drag is calculated in terms of the jump in entropy $[\![s]\!]$:

$$[\![s]\!] \simeq -M_\infty^2 \frac{(\gamma + 1)}{12} u^3. \tag{7}$$

In Reference 4, it is shown that imposing (6) across the shock is equivalent to modifying the flux according to

$$f_d - f_u = (\Delta s/R) f_d. \tag{8}$$

Therefore the shock is weakened due to a source distribution of strength proportional to the jump in entropy.

The purpose of the present work is to replace these shock fitting methods with a conservative calculation procedure, where shocks are numerically captured. The flux, including entropy effects, can be approximated by

$$\begin{aligned} \rho(1 + u) = \mathrm{e}^{-\Delta s/R}\{1 + (1 - M_\infty^2)u - \tfrac{1}{2}M_\infty^2 u^2[3 - (2 - \gamma)M_\infty^2] \\ + M_\infty^2[-\tfrac{1}{2} + (2 - \gamma)M_\infty^2 - (2 - \gamma)(3 - 2\gamma)M_\infty^4 u^3/6]\} + \cdots \end{aligned} \tag{9}$$

The momentum becomes

$$p(1 + u)u + p = \mathrm{e}^{-\Delta s/R}\left\{\frac{1}{\gamma M_\infty^2} + (1 - M_\infty^2)\frac{u^2}{2}[1 - \tfrac{1}{3}(2 - \gamma)M_\infty^2]M_\infty^2 u^3\right\} + \cdots \tag{10}$$

Eliminating $\mathrm{e}^{-\Delta s/R}$ in expression (9) using (10) leads to a modified small disturbance equation of the following conservative form:

$$[(1 - M_\infty^2)\phi_x - \tfrac{1}{2}M_\infty^2\{(\gamma + 1) + 2(1 - M_\infty^2)\}\phi_x^2 + \tfrac{1}{2}M_\infty^2(\gamma + 1)\phi_x^3]_x + \phi_{yy} = 0 \tag{11}$$

Strictly speaking, other terms of the expansion of the y-component of the flux should be included for consistency, for example ϕ_{yx}^2 and $(\phi_y\phi_x)_y$ are of the same order as ϕ_x^3, i.e. (τ^2). Nevertheless equation (11) represents an improvement over the classical equation (2). In particular the jump condition admitted by the weak solution of equation (11) is a second-order approximation of the Prandtl relation. In addition, equation (11) changes type (elliptic to hyperbolic) at a speed closer to the exact sonic condition.

An equivalent form of equation (11) is

$$F_x + \phi_{yy} = 0, \tag{12}$$

where

$$F = f(1 - \phi_x),$$
$$f = (1 - M_\infty^2)\phi_x - \tfrac{1}{2}M_\infty^2(\gamma + 1)\phi_x^2.$$

Obviously F is no longer a quadratic function of ϕ_x since the shock is no longer isentropic and equations (11) and (12) do not admit a similarity solution. In a calculation based on a conservative difference approximation of equation (12), the need for evaluating entropy production across a shock would be eliminated. These concepts are extended to the full potential equation in the following sections.

TRANSONIC FULL POTENTIAL EQUATION

Quasi-one-dimensional flows

Consider internal flows in a nozzle with a variable area distribution. The governing equations of continuity, momentum and energy for this Quasi-1D problem are

$$(\tilde{\rho}Au)_x = 0, \tag{13}$$

$$(A\rho u^2 + Ap)_x - A_x p = 0, \tag{14}$$

$$(\rho u A H_\infty)_x = 0; \quad H_\infty = \frac{\gamma p}{(\gamma - 1)\rho} + \frac{1}{2}u^2. \tag{15}$$

$\tilde{\rho}$ represents the artificial compressibility necessary for the calculations of transonic flows:

$$\tilde{\rho} = \rho - \mu(\rho_e - \rho_{e-1}) \tag{16a}$$

$$\mu = \max\left[0, 1 - \frac{1}{M^2}, 1 - \frac{1}{M_{e-1}^2}\right] \tag{16b}$$

There is no loss of generality, in the 1-D case, to assume that, in terms of a potential (Φ)

$$u = \Phi_x, \tag{17a}$$

and hence equation (13) becomes

$$(\tilde{\rho}A\Phi_x)_x = 0. \tag{17b}$$

Because vorticity does not exist for one-dimensional flows, the present model is exact. The pressure is obtained by satisfying a second-order form of the momentum equation. Assuming the potential, Φ, to be defined at the nodes, and the pressure, p, density, ρ, and the speed, u, to be defined at the mid-cells, a central difference approximation of equation (14) at node j reads: (see Figure 1(a)).

$$(A\rho u^2 + Ap)_{j+1/2} - (A\rho u^2 + Ap)_{j-1/2} - \tfrac{1}{2}(A_{j+1/2} - A_{j-1/2})(p_{j+1/2} + p_{j-1/2}) = 0 \tag{18}$$

Similarly, at node $(j-1)$,

$$(A\rho u^2 + Ap)_{j-1/2} - (A\rho u^2 + Ap)_{j-3/2} - \tfrac{1}{2}(A_{j-1/2} - A_{j-3/2})(p_{j-1/2} + p_{j-3/2}) = 0 \tag{19}$$

Subtracting (18) from (19), a tridiagonal matrix for the pressure is obtained. With the pressure and velocity known, the density can be determined from the energy equation (15).

The boundary conditions for the tridiagonal system are the prescribed exit pressure and a Neumann condition at the inlet in the form of equation (18), assuming the density ρ and the speed u to be lagged from the previous iteration.

Similarly, a finite element implementation is straightforward, especially that the Neumann condition for pressure in this case turns out to be the natural boundary condition of the system. This interesting point is important and will be demonstrated in the next section on 2-D flows.

Numerical results for the nozzle problem of Figure 1(b) are presented in Figure 1(c) and compared to the exact Euler solution.

Two-dimensional flows: non-lifting aerofoils

Transonic flows around a symmetric (NACA 0012) aerofoil at zero angle of attack are calculated using the present formulation. The governing equations are

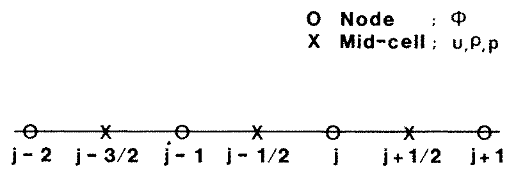

Figure 1(a). Finite Difference Grid for a Quasi-1D Calculation

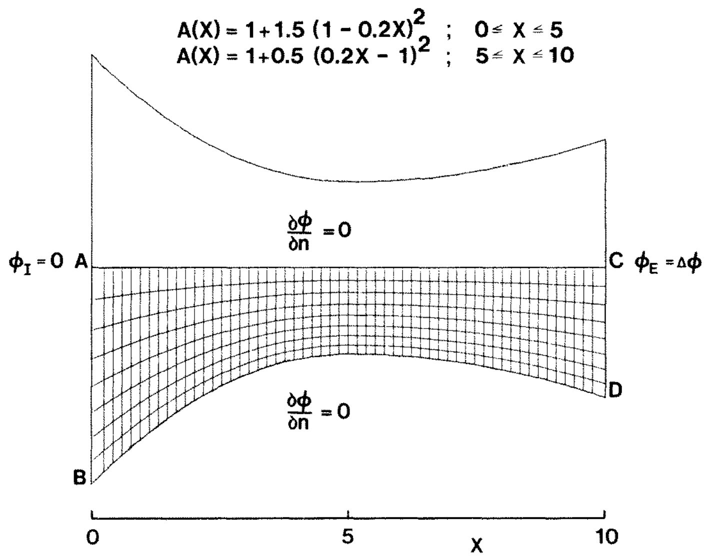

Figure 1(b). Nozzle Shape for Quasi-1D Calculations

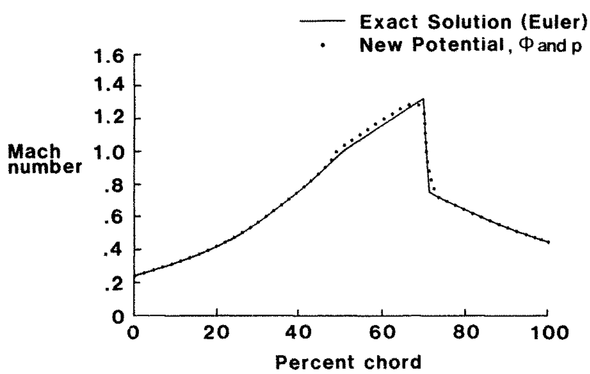

Figure 1(c). Mach Number Distribution in Nozzle

$$\nabla \cdot (\tilde{\rho} \nabla \Phi) = 0, \tag{20}$$

$$\nabla^2 p = -(\rho u^2)_x - (\rho uv)_{yx} - (\rho uv)_{xy} - (\rho v^2)_{yy} \equiv f_x + g_y, \tag{21a}$$

obtained by taking the divergence of the x and y momentum equations:

$$p_x = -[(\rho u^2)_x + (\rho uv)_y] \equiv f, \tag{21b}$$

$$p_y = -[(\rho v^2)_y + (\rho uv)_x] \equiv g. \tag{21c}$$

The losses P_L are obtained by calculating the ratio of the pressure from equation (21a) to the ideal pressure,

$$p_i = \left[1 - \frac{\gamma - 1}{2} M_\infty^2 (\Phi_x^2 + \Phi_y^2 - 1)\right]^{\gamma/\gamma - 1} \Big/ \gamma M_\infty^2, \tag{22a}$$

$$P_L = p/p_i \equiv e^{-\Delta s/R}, \tag{22b}$$

and the density is calculated as

$$\rho = \rho_i P_L = \left[1 - \frac{\gamma - 1}{2} M_\infty^2 (\Phi_x^2 + \Phi_y^2 - 1)\right]^{(1/\gamma - 1)} P_L. \tag{23}$$

Equation (21a) is of mixed type since the right-hand side can be written as $M^2 p_{ss} + f(\rho, u, v)$; hence

$$(1 - M^2) p_{ss} + p_{nn} = f(\rho, u, v). \tag{24}$$

To understand the boundary conditions on equation (21a), it is useful to demonstrate the finite element or weighted residual discretization of the equation. Multiplying by a weight function W, and integrating over the solution domain:

$$\iint W[p_{xx} - f_x + p_{yy} - g_y] \mathrm{d}x\mathrm{d}y = 0. \tag{25}$$

Integrating by parts yields

$$\iint \{W_x[p_x - f] + W_y[p_y - g]\} \mathrm{d}x\mathrm{d}y - \int_c W(p_x - f)\mathrm{d}y - \int_c W(p_y - g)\mathrm{d}x = 0. \tag{26}$$

The contour integrals are nothing but the momentum equations (21b, c) that must vanish. Over any contours where p is not specified, say over the aerofoil or at the exit, the natural boundary condition is the vanishing of the contour integral. Far upstream the pressure is taken to be p_∞.

It is assumed here that a fine mesh in the neighbourhood of a shock is used and hence, owing to the effect of the artificial viscosity in the velocity calculations, the pressure is considered to be a continuous function with a large gradient. This means that a shock will be smeared over a number of elements and that sharp shocks must be calculated using fine meshes, as in most conservative calculations. One might comment that in the classical potential conservative calculation sharp shocks are sometimes captured within very few elements; for example, normal shocks are captured in two elements because, in this case, shock capturing methods are very close to shock fitting.[6] For oblique supersonic/supersonic shocks, however, in all the existing conservative potential calculations as well as in Euler calculations shocks are smeared over many elements.

To solve equation (20), the artificial compressibility method can be easily applied.[5] Necessary modifications to guarantee the convergence of standard relaxation procedures for mixed-type equations, independent of the artificial viscosity, are also needed as discussed in the same reference. Numerical results based on the proposed formulation are shown in Figure 2 for subsonic flows and compared to the classical potential solution; the agreement is excellent. Bilinear four-node finite elements are used for all two-dimensional calculations.

In Figure 3, results for transonic flows are demonstrated for $M_\infty = 0{\cdot}85$. The shock in the present calculation is weaker and is positioned upstream of the isentropic shock. There is, however, a slight discrepancy between the two solutions in the smooth acceleration region upstream of the shock due to the numerical accuracy in the calculations of the losses. In the present computations, owing to computer core limitations, only 896 elements are used with 45 points on the aerofoil. Better agreement in this region is expected if finer meshes were used.

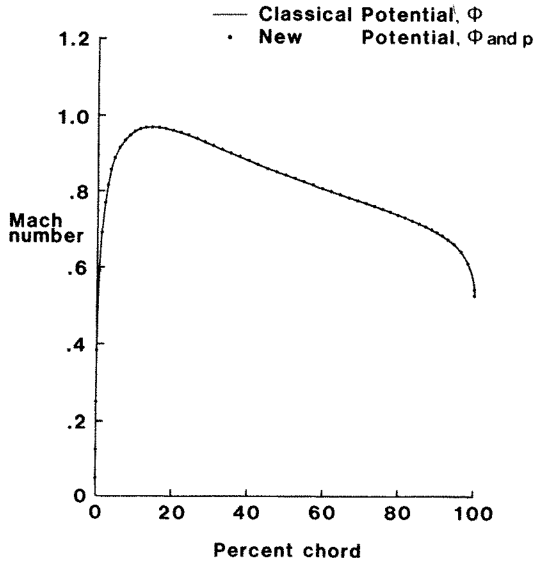

Figure 2. FEM Solution of Subsonic Non-lifting Flow around NACA 0012 aerofoil, $M_\infty = 0{\cdot}72$, Classical Potential and New Potential

Two-dimensional flows: lifting aerofoils

In the classical potential lifting formulation, a jump in $(\Delta\Phi)$ must be imposed across a cut while pressure, density and speed are continuous across this cut. On the other hand, in the Euler calculations only the pressure is continuous across the wake, whereas the density and the tangential velocity have a jump (contact discontinuity).

In the present model, the wake is treated as in the potential calculations: the circulation $\Gamma = \Delta\Phi$ is determined such that at the trailing edge, the speeds (q_{up}) at the upper surface and (q_{lo}) at the

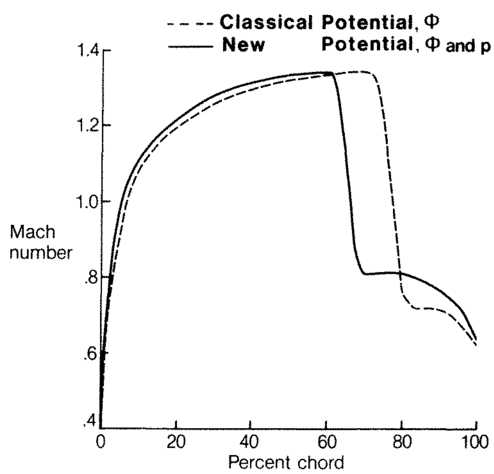

Figure 3. FEM Solution of Transonic Non-lifting Flow around NACA 0012 aerofoil, $M_\infty = 0{\cdot}85$, Classical Potential and New Potential

lower surface are equal. The following iterative procedure is used:

$$\Gamma^{n+1} = \Gamma^{n} + \beta(q_{\mathrm{up}} - q_{\mathrm{lo}}), \tag{27}$$

where β is a properly chosen relaxation parameter. The far field behaviour consists of a vortex of strength proportional to $\Gamma = \Delta\Phi$.

For subsonic flows, the results of the present model agree very well with the classical potential solution as shown in Figures 4 and 5.

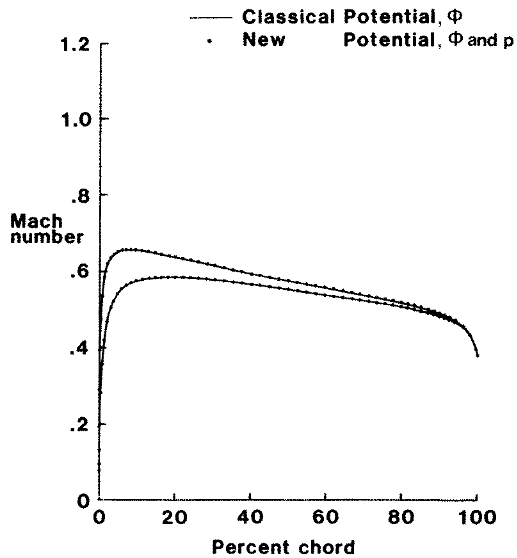

Figure 4. FEM Solution of Subsonic Lifting Flow around NACA 0012 aerofoil, $M_{\infty} = 0{\cdot}5$, $\alpha = 1°$, Classical Potential and New Potential

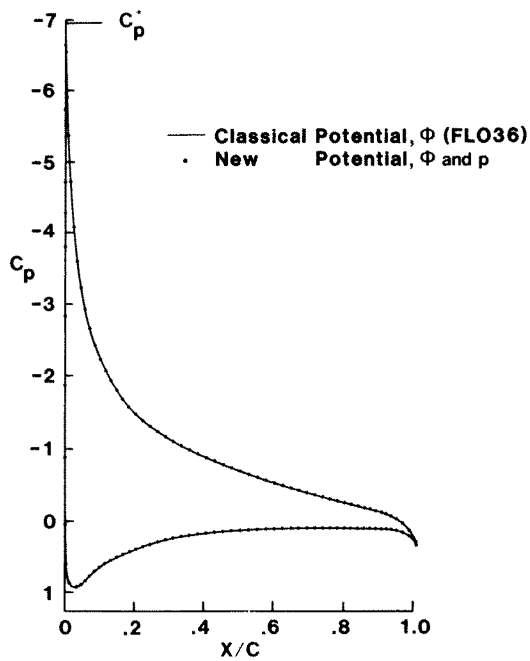

Figure 5. FEM Solution of Subsonic Lifting Flow around NACA 0012 aerofoil, $M_{\infty} = 0{\cdot}3$, $\alpha = 10°$ Classical Potential and New Potential

If shocks develop, at higher free-stream Mach numbers and/or higher angles of attack, the present results should agree with neither the potential nor the Euler solutions. In Figure 6, the surface Mach number distribution is shown for $M_\infty = 0{\cdot}83$ and $\alpha = 0{\cdot}1°$. At this latter condition, the classical potential solution is not unique.[7,8] The non-isentropic model produces however a unique solution as discussed in Reference 5. The present conservative calculations are shown in Figure 7 superposed on a Figure from Reference 8. It seems that in these calculations, as well as in the shock fitting calculations of Reference 4, the non-uniqueness problem discovered by Steinhoff and Jameson[7] is circumvented, at least for this numerical example.

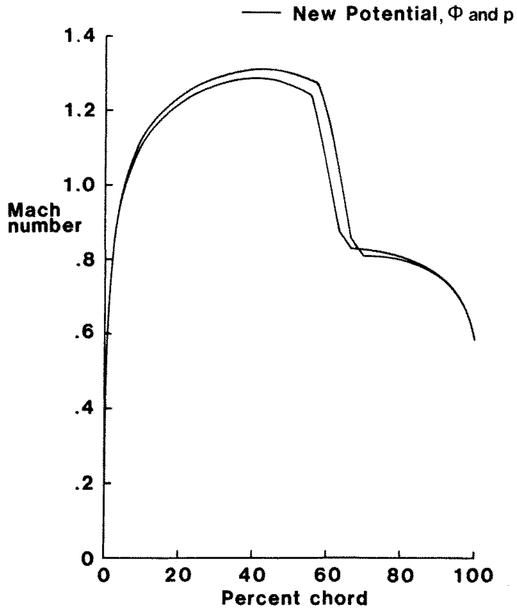

Figure 6. FEM Solution of Transonic Lifting Flow around NACA 0012 aerofoil, $M_\infty = 0{\cdot}83$, $\alpha = 0{\cdot}1°$, Classical Potential and New Potential

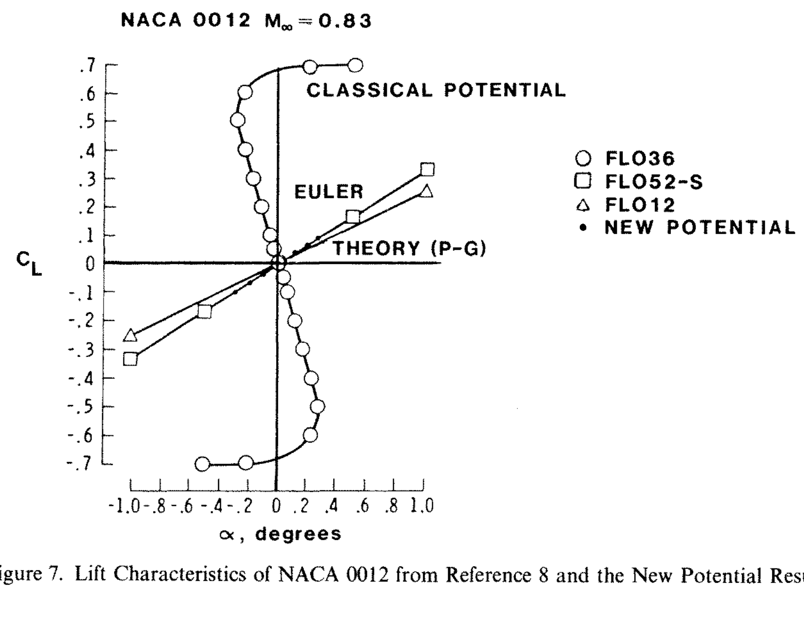

Figure 7. Lift Characteristics of NACA 0012 from Reference 8 and the New Potential Results.

CONCLUDING REMARKS

Conservative calculations of non-isentropic flows are demonstrated using a modified potential formulation and a second-order mixed-type equation for the pressure. The pressure equation is demonstrated to have very simple boundary conditions. Examples of lifting aerofoils at transonic speeds are shown. The non-isentropic effects are sometimes appreciable and in some cases are crucial for obtaining a unique solution.

Applications of the present method to other aerodynamic configurations, for example internal turbomachinery flows, are in progress. If the vorticity effects are important, the present formulation can be extended to allow for rotational flows using a perturbation stream function of similar form to the potential equation. In this case the vorticity has to be calculated in terms of the gradient of losses normal to the streamline direction and such calculations would thus be equivalent to solving the Euler equations.

ACKNOWLEDGEMENTS

The authors would like to thank the Engineering Staff of Pratt & Whitney Canada for their assistance with some of the calculations. This research was supported by Contract PRAI-P-8219 and Grant A-3662 of the Natural Sciences and Engineering Research Council of Canada (NSERC) and by Pratt & Whitney Canada Inc.

NOMENCLATURE

A	= nozzle area
a	= speed of sound
c	= aerofoil chord
C_L	= lift coefficient
f, F	= mass flux
H	= enthalpy
M	= Mach number
M	= momentum
p	= static pressure
P_L	= total pressure loss
q	= velocity, $\sqrt{(u^2 + v^2)}$
R	= gas constant
s	= entropy
u, v	= velocity components
x, y	= Cartesian co-ordinates
α	= angle of attack
β	= relaxation factor
γ	= isentropic exponent
Γ	= circulation
Δ	= increment
ρ	= density
ϕ	= perturbation potential
Φ	= full potential
μ	= artificial viscosity coefficient
ω	= vorticity
τ	= aerofoil thickness ratio

Subscripts

d	= downstream
e	= element
$e-1$	= upstream element
i	= ideal
j	= nodal
$j+\frac{1}{2}, j-\frac{1}{2}$	= mid-cell
lo	= trailing edge, lower surface
s, n	= streamline direction and normal to it, respectively
u	= upstream
up	= trailing edge, upper surface
x, y	= differentiation, w.r.t. x and y
∞	= free-stream condition

Superscripts

*	= sonic
$\sim$	= artificial density

Other symbols

$[\![\ ]\!]$	= jump of quantity across shock
$\langle\ \rangle$	= average of quantity across shock

REFERENCES

1. E. Murman and J. Cole, 'Inviscid drag at transonic speeds', *AIAA Paper 74–540*, 1974.
2. J. Steger and B. Baldwin, 'Shock waves and drag in the numerical calculation of isentropic transonic flow', *NASA TN D-6997*, October 1972.
3. M. Hafez and D. Lovell, 'Transonic small disturbance calculations including entropy corrections', *Symposium on Numerical and Physical Aspects of Aerodynamic Flows*, California State University, Long Beach, California, 1981.
4. M. Hafez and D. Lovell, 'Entropy and vorticity corrections for transonic flows', *AIAA Paper No. 83–1926*, 1983.
5. W. G. Habashi and M. Hafez, 'Finite element solutions of transonic flow problems', *AIAA Journal*, **20,** (10), 1368–1376 (1982).
6. S. Osher, M. Hafez and W. Whitlow, 'Entropy satisfying approximations for the full potential equation of transonic flow', submitted to *Math. Comp.*, 1983.
7. J. Steinhoff and A. Jameson, 'Multiple solutions of the transonic potential flow equation', *AIAA Journal*, **20,** (11), 1521–1525 (1982).
8. M. D. Salas, A. Jameson and R. E. Melnik, 'A comparative study of the nonuniqueness problem of the potential equation', *NASA Technical Paper 2385*, January 1985.